Calculations of Complex Chemical Reaction Equilibria using Free Energy Minimization and Arc-Length Continuation

Housam Binous[1†] and Ahmed Bellagi[2]

[1] Chemical Engineering Department, National Institute of Applied Sciences & Technology, University of Carthage, Tunisia.

[2] Energy Engineering Department, Ecole Nationale d'Ingénieurs de Monastir - ENIM, University of Monastir, Tunisia.

†corresponding author: binoushousam@yahoo.com

Abstract

In the present paper, we determine the chemical equilibrium compositions for two combustion reactions involving either hydrazine or propane at fixed high pressure and temperature values using several computational approaches. Then, we compute the chemical equilibria for reacting systems under a multitude of temperature and pressure conditions and various initial system compositions. These sensitivity analyses are based on a combination of the method of Lagrangian multipliers and the arc-length continuation technique. Indeed, three industrially relevant case studies are elucidated: (1) the synthesis of ammonia using the Haber process, (2) the gasification of a typical biomass surrogate: glucose using steam and (3) the gasification of cellulose using steam. For all the above reacting systems, our results are benchmarked against their counterparts obtained either from the ubiquitous process simulator: ASPEN-Plus® or from data available in the open literature.

Keywords

Complex chemical reaction equilibria, arc-length continuation, Haber synthesis, Gasification process, glucose, cellulose, Peng Robinson Equation of State, Syngas production, MATHEMATICA© and ASPEN-PLUS®.

1. Introduction

Calculation of complex chemical equilibria has been for decades –and remains in some cases even nowadays– a huge challenge. The fields, where accurate knowledge of chemical equilibria is necessary, encompass high temperature and pressure reactions, design of explosives, development of rocket propellants, design and conception of new chemical processes, combustion, biomass gasification, etc.

Calculations of chemical equilibria are performed in order to [1]

- Determine the equilibrium composition of mixtures (mole or mass fractions, concentrations, partial pressures, etc.) for fixed operating conditions (e.g., reactants composition, temperature and pressure), or
- Investigate the evolution of the equilibrium compositions when the operating conditions are varied.

Different mathematical and numerical techniques are available for the calculations of chemical equilibria at fixed initial values of reactants' composition, temperature and pressure:

- Techniques for the resolution of a set of non-linear algebraic equations (equilibrium constant method, minimization of Gibbs free energy combined with Lagrangian multipliers for equality constraints in order to reduce the constrained minimization problem to a set of nonlinear algebraic equations), and
- Optimization techniques (direct minimization of Gibbs free energy).

The objective of the present paper is to illustrate the calculation of complex chemical equilibria using different mathematical and numerical approaches. Hydrazine and propane combustion at high temperature and pressure are used to illustrate both group of methods. For the sensitivity analyses of the equilibrium state when one of the following parameters –initial reactants' composition, temperature or pressure– is varied, we study the following three cases: the Haber ammonia process and the cellulose and glucose gasification. Arc-length continuation technique is applied to this purpose.

Appendix A provides the reader with some background information on useful chemical engineering thermodynamics. In fact, we give a concise description of the Peng-Robinson equation of state (PR-EoS) used in the sensitivity analyses to describe the volumetric behavior of gas mixtures under high pressure and to deduce the corresponding residual

Gibbs free energy of such systems. Appendix B gives a full description of the application of arc-length continuation in order to perform various parametric studies for chemically reacting systems.

In the following, readers are first exposed to the numerical methods used to determine the equilibrium compositions of any reacting system. For researchers involved with catalyst development, these equilibrium values represent the targets that ideally one should achieve. In this section, we also formulate the mathematical problem (i.e., a minimization of the Gibbs free energy of mixtures under few appropriate equality constraints) and indicate how we will attempt to solve this minimization problem. The third section illustrates by two examples, hydrazine and propane combustion under high pressure and temperature conditions, the methods and techniques used to calculate complex chemical equilibria either directly by minimizing the free enthalpy of the product gaseous mixture or by applying the Lagrangian multiplier algorithm. The fourth section incorporate three case studies, which are elucidated thoroughly using the Lagrangian multiplier approach combined with the arc-length continuation technique. We will not only provide equilibrium compositions for several industrially relevant systems but also perform sensitivity analyses by varying one of the following parameters: temperature, pressure, initial composition of the reacting species… One such gaseous reacting system pertains to the Haber process where nitrogen from the cryogenic separation of air constituents is reacting with hydrogen derived from natural gas steam reforming to produce ammonia. The next two examples stem from a currently very active research area: biomass gasification. In fact, we consider two biomass surrogates: glucose and cellulose. We predict the equilibrium compositions for their gasification using steam as the oxidizing agent. Finally, we end this paper with some concluding remarks relevant to the academic and industrial scope of the calculation methodology and results described herein. We also direct interested readers to possible extensions of the present treatise.

2. Gibbs Free-Energy Minimization Method

In order to estimate the equilibrium composition at fixed temperature and pressure of a complex chemical system composed of several known components and subject (or not) to a certain number of constraints, the appropriate method is the minimization of the mixture Gibbs free energyG_M [2, 3],

$$min\, G_M(n_i) \tag{1}$$

Since this state function depends on the number of moles n_i of each of the involved chemical species i, these latter quantities can be taken as decision variables. This is a constrained minimization problem: The set of n_i −¿values that minimize G_M must verify equality constraints expressing the conservation of the atomic elements. Denoting with α_{ki} the number of element k in the chemical formula of component$i$ and with φ_k the total number of moles of element k initially present in the feed, these equality constraints write

$$\sum_i n_i \alpha_{ik} = \varphi_k \tag{2}$$

Another constraint must be considered when the real fluid equation of state is used to describe the volumetric behavior of the equilibrium mixture. If one adopts the Peng-Robinson equation of state (PR EoS) to this purpose, the constraint writes

$$f_Z = Z^3 + (b_M - 1) Z^2 + (a_M - 3b_M^2 - 2b_M) - a_M b_M + b_M^2 + b_M^3 = 0 \tag{3}$$

Where $Z = Pv/RT$ is the compressibility factor.

Because we are dealing with only equality constraints, the optimum solution can be obtained by introducing the Lagrangian multipliers, noted byλ_k for the w chemical elements, and λ_Z for the compressibility factor. The problem at hand consists now in minimizing the Lagrangian function L defined as:

$$L = G_M(n_i) + \sum_{k=1..w} \lambda_k \left[\left(\sum_{i=1..N} n_i a_{ik} \right) - \varphi_k \right] + \lambda_Z f_Z \tag{4}$$

The minimization problem is thus converted into the following system of $(w+N+2)$ nonlinear equations [3]:

$$\begin{cases} \left(\dfrac{\partial L}{\partial \lambda_k} \right)_{n_i, Z, \lambda_{j \neq k}, \lambda_Z} = 0 \quad (k = 1, 2, 3, \ldots, w) \\ \left(\dfrac{\partial L}{\partial \lambda_Z} \right)_{n_i, Z, \lambda_k} = 0 \\ \left(\dfrac{\partial L}{\partial n_i} \right)_{n_{k \neq i}, Z, \lambda_k, \lambda_Z} = 0 \quad (i = 1, 2, 3, \ldots, N) \\ \left(\dfrac{\partial L}{\partial Z} \right)_{n_i, \lambda_k, \lambda_Z} = 0 \end{cases} \tag{5}$$

The unknowns in the above system are the N number of moles present in the system (i.e.,n_i for$i = 1, 2, 3, \ldots, N$), the compressibility factor (i.e.,Z) and $(w+1)$ Lagrangian multipliers (i.e., λ_k for $k = 1, 2, 3, \ldots, w$ andλ_Z).

In order to compute the Gibbs free energy for a multi-phase system, the Gibbs free energy of all phases are added [3]. We can subdivide the contributions into two main parts:

i. Gibbs free energy for the gas and liquid phases. In fact, the calculation of both of these terms involves applying the PR EoS and taking either the liquid or gas phase molar volume (or equivalently the liquid or gas phase compression factor).
ii. Gibbs free energy of the solid phase.

Gas and Liquid phase mixture Gibbs free energy

The advantage of the usage of a cubic EoS, such as the PR EoS, lays in the fact that the liquid and gas phase mixtures can be dealt with in a similar fashion by just using the corresponding value of the molar volume or the compressibility factor.

For the gas-phase, the free energy of the mixture, $G_{g,M}$, is the sum of the ideal gas contributions, $G^{o}_{g,M}$, and the residual contributions, G^{R}_{M} [4]:

$$G_{g,M} = G^{o}_{g,M} + G^{R}_{M} \tag{6}$$

$G^{o}_{g,M}$ is given by:

$$G^{o}_{g,M} = n\sum_{i=1}^{n} y_i\left(g^{o}_{i} + RT\ln y_i\right) \tag{7}$$

In the above equation, the pure component molar ideal gas Gibbs free energy or g^{o}_{i} is expressed by:

$$g^{o}_{i} = g^{o}_{i}(To) + \int_{To}^{T} C_{p,i}\,dT - T\int_{To}^{T}\frac{C_{p,i}}{T}dT + -S_i(To)(T-To) + RT\ln\left(\frac{P}{P^{o}}\right) \tag{8}$$

It is usual to take $To = ¿$ 298.15 K and $P^{o} = 1\,¿$as reference temperature and pressure, respectively.

It should be noticed that all of the terms on the right hand side of the above equation (i.e., definingg^{o}_{i}) are functions of the temperature except the last one, which contains also a pressure-dependency.

Although it is possible to use the above expression in order to calculateg^{o}_{i}, we chose a different route in the present paper. Indeed, we fit the experimental values of g^{o}_{i} versus T *at* $P^{o} = 1\,¿$. Such values are available in several sources of thermochemical data of pure substances (e.g., Ref. [5]). For the sensitivity analysis of the equilibria treated in the

following, analytical expressions for $g_i^o(T,P^o)$ are needed, so we select the following empirical expression for $g_i^o(T,P^o)$:

$$g_i^o(T,P^o)=a_0+a_1T+a_1T^2+a_1T^3+a_1T^4+a_5T^5+a_6T^6+a_7T^7+a_8T^8+a_9T\ln(T) \quad (9)$$
$$+a_6T^6+a_7T^7+a_8T^8+a_9T\ln(T)$$

Finally, we include the pressure-dependency:

$$g_i^o(T,P)=g_i^o(T,P^o)+RT\ln(P/P^o) \quad (10)$$

It should be noted that the parameters $\{a_i, i=1..9\}$ are determined separately for every pure component of the chemical system under study using the same platform of computation (i.e., `FindFit` of MATHEMATICA©).

Solid Phase Gibbs free energy

Because solid-solid interactions are generally negligible, the total Gibbs free energy of a solid phase is merely the sum of all contributions from each component existing in the solid phase considered as present alone. Hence, the equation below applies:

$$n_s g_{s,M}=\sum_j n_{j,s}g_{j,s} \quad (11)$$

In addition, the Gibbs free energy of any solid species (e.g., carbon in the case of gasification of biomass) is taken as a function of temperature only. In fact, this solid phase property is not strongly affected by pressure. Here, we make use again of the experimental thermochemical data available in Ref. [5]. For carbon, data of $g_{C,s}$ versus T allow us to generate an interpolating function using the built-in command of MATHEMATICA© called `Interpolation`.

Finally, the expression of the total Gibbs free energy of a system with gas and solid phases writes as follows:

$$G^{total}=n_g g_{g,M}+n_s g_{s,M} \quad (12)$$

3. Complex Chemical Equilibria Calculation Methods

We illustrate these calculation methods with two case studies: hydrazine and propane combustion.

3.1. Hydrazine combustion

Hydrazine, with the chemical formula N_2H_4, is primarily used as foaming agent in the preparation of polymer foams. It is also employed to reduce the concentration of dissolved oxygen, a source of corrosion, in the boilers of large conventional or nuclear power plants. A further application of hydrazine is as rocket fuel. Rocket engines are often fueled with this monopropellant in the last descent step of spacecraft (e.g., Curiosity and Perseverance rover landing on Mars in 2012 and February 2021, respectively). In these cases, hydrazine is catalytically decomposed into its elements: oxygen and nitrogen. This exothermic reaction produces a huge amount of gas, and high pressure, from a small volume of liquid.

The present illustration does not investigate the catalytic decomposition of hydrazine but rather its combustion with pure oxygen at high temperature (3500 K) and pressure (51 bar). The gaseous product mixture involves many species from molecular compounds to atomic elements and radicals. The equilibrium composition of a mixture of 10 species (H, H_2, N, N_2, O, O_2, H_2O, NO, NH and OH) was calculated using the minimization of the Gibbs free energy of the reacting of the chemical species [6]. Two numerical procedures were applied for the solution: steepest descent and linear programming.

In the following, we include two more species, NO_2 and NH_2, to the system and solve the problem applying three different methods using MATHEMATICA©.

3.1.1 Lagrangian Multipliers Method and Element Potentials

Assuming ideal gas behavior of the reacting mixture, the problem at hand consists in finding the mole numbers of the twelve species n_i that minimize the Gibbs free energy of the gaseous mixture $G_M(T, P, n_i)$,

$$G_M(T, P, n_i) = G_M(T, P^o, n_i) + RT \ln\left(\frac{P}{P^o}\right) \tag{13}$$

$G_M(T, P^o, n_i)$ is the Gibbs free energy at temperature T and reference pressure P^o (e.g., 1 bar),

$$G_M(T, P^o, n_i) = \sum_{i=1}^{12} n_i \mu_i^o(T, P^o) \tag{14}$$

where $\mu_i^o(T, P^o)$ is the chemical potential of specie *i* at T and P^o,

$$\mu_i^o(T, P^o) = g_i^o(T, P^o) + RT \ln(y_i) \tag{15}$$

$g_i^o(T,P^o)$ is the molar free energy of the pure specie i and y_i is its molar fraction in the mixture.

The solution mole numbers n_i minimizing G_M are subject to the constraints of elements conservation.

For an equimolar mixture of reactants (oxygen and hydrazine), these constraints write:

- Oxygen balance

$$f_O = 2 - (y_O + 2y_{O2} + y_{NO} + y_{H2O} + y_{OH} + 2y_{NO2})n = 0 \quad (16)$$

With

$$n = \sum_{i=1}^{12} n_i \quad (17)$$

- Hydrogen balance

$$f_H = 4 - (y_H + 2y_{H2} + y_{NH} + 2y_{H2O} + y_{OH} + 2y_{NH2})n = 0 \quad (18)$$

- Nitrogen balance

$$f_N = 2 - (y_N + 2y_{N2} + y_{NH} + y_{NO} + y_{NO2} + y_{NH2})n = 0 \quad (19)$$

The Lagrangian function of the mixture can be expressed as follows

$$L = G_M(T,P,n_i) - \lambda_O f_O - \lambda_H f_H - \lambda_N f_N \quad (20)$$

$\lambda_O, \lambda_H \wedge \lambda_H$ are the Lagrange multipliers. We obtain by minimizing L in respect to n_i the following set of very interesting expressions for the chemical potentials of the mixture components at equilibrium,

$$\mu_O(T,P,n_i) = \lambda_O$$
$$\mu_{O2}(T,P,n_i) = 2\lambda_O$$
$$\mu_H(T,P,n_i) = \lambda_H$$
$$\mu_{H2}(T,P,n_i) = 2\lambda_H$$
$$\mu_N(T,P,n_i) = \lambda_N$$
$$\mu_{N2}(T,P,n_i) = 2\lambda_N$$

$$\mu_{H2O}(T,P,n_i) = 2\lambda_H + \lambda_O$$
$$\mu_{NH}(T,P,n_i) = \lambda_N + \lambda_H$$
$$\mu_{NH2}(T,P,n_i) = \lambda_N + 2\lambda_H$$
$$\mu_{NO2}(T,P,n_i) = \lambda_N + 2\lambda_O$$
$$\mu_{NO}(T,P,n_i) = \lambda_N + \lambda_O$$
$$\mu_{OH}(T,P,n_i) = \lambda_O + \lambda_H$$

These relations suggest that the Lagrange multipliers can be considered as element potentials [7], for the chemical potential of every compound is equal to the sum of the potentials of its constituting elements affected with factors corresponding to its chemical formula. Further,

these element potentials – for each chemical element there is only one potential – together with the total number of moles of the mixture are the only unknowns of the problem, regardless the number of chemical species present.

We can now express the mole fraction of each of these species as function of the appropriate Lagrange multipliers, for instance, for H_2O and OH:

$$y_{H2O} = \exp\left[\frac{-g_{H2O}(T,P) + 2\lambda_H + \lambda_O}{RT}\right] \tag{21}$$

or

$$y_{OH} = \exp\left[\frac{-g_{OH}(T,P) + \lambda_H + \lambda_O}{RT}\right] \tag{22}$$

After replacing the mole fractions by their expressions in the linear constraint relations and adding the summation equation:

$$\sum_{i=1}^{12} y_i = 1 \tag{23}$$

we obtain a set of *only* four algebraic equations in four variables λ_H, λ_O, λ_N and n that can readily be solved using the MATHEMATICA© function `FindRoot`. The results for $T = 3500\,K$ and $P = 51$ ¿ are given in Table 1. In the last column, we give, for the sake of comparison, the compositions reported in Ref. [6] obtained at the same conditions. As already mentioned, NH_2 and NO_2 were not included in the gaseous mixture considered in that reference, their actual compositions are effectively very small, 3.92 10^{-6} and 10^{-5} respectively, so that they have little effect on the mole fractions of the remaining species. For eight of the 10 mixture components the results of the present calculations are in good agreement with those of Ref. [6]. For the species N and NH, the noticed discrepancy is attributed to the more recent values of $g_i^o(T,P^o)$ used here, calculated basing on enthalpy and entropy formulae from NIST webbook [8].

Species	y_i	$g_i^o(T,P^o)/RT$	y_i [6]
N	0.00002	-6.06608	0.00086
O	0.01010	-14.7444	0.01095

H	0.02465	-10.1769	0.02482
NH	$4.35\ 10^{-6}$	-14.6569	0.00042
NO	0.01627	-28.3447	0.01672
NH_2	$3.92\ 10^{-6}$	-24.501	---------
H_2O	0.47846	-38.4983	0.47800
O_2	0.02156	-30.9105	0.02277
N_2	0.29731	-28.9657	0.29617
H_2	0.08867	-21.4048	0.09015
OH	0.06295	-26.5222	0.05913
NO_2	0.00001	-36.6686	---------

Table 1 – Equilibrium composition of the product gas for hydrazine combustion.

3.1.2 Mass Action Method

The same problem can be solved using the traditional equilibrium constant method. Possible routes to the product species involved in the hydrazine combustion process might be the transformations described by the reactions 1-9 in Table 2.

Reaction	Equilibrium Constant $K_j(T,P)$
$H_2 \rightleftharpoons 2H$	$K_1(T) = \frac{y_H^2}{y_{H_2}} P$

$O_2 \rightleftharpoons 2O$	$K_2(T)=\frac{y_O^2}{y_{O_2}}P$
$N_2 \rightleftharpoons 2N$	$K_3(T)=\frac{y_N^2}{y_{N_2}}P$
$2H_2O \rightleftharpoons 2H_2+O_2$	$K_4(T)=\frac{y_{H_2}^2 y_{O_2}}{y_{H_2O}^2}P$
$2H_2O \rightleftharpoons H_2+2OH$	$K_5(T)=\frac{y_{OH}^2 y_{H_2}}{y_{H_2O}^2}P$
$N_2+O_2 \rightleftharpoons 2NO$	$K_6(T)=\frac{y_{NO}^2}{y_{N_2}y_{O_2}}$
$N_2+2O_2 \rightleftharpoons 2NO_2$	$K_7(T)=\frac{y_{NO_2}^2}{y_{N_2}y_O^2P}$
$N_2+H_2 \rightleftharpoons 2NH$	$K_8(T)=\frac{y_{NH}^2}{y_{N_2}y_{H_2}}$
$\frac{1}{2}N_2+H_2 \rightleftharpoons NH_2$	$K_9(T)=\frac{y_{NH_2}}{\sqrt{y_{N_2}}y_{H_2}\sqrt{P}}$

Table 2 – Reactions and equilibrium constants (hydrazine combustion).

The equilibrium constant $K_j(T)$ of a reaction (j) is related to its molar reaction Gibbs energy $\Delta_j G^0(T)$ at standard pressure P^o as follows

$$K_j(T)=\exp\left[\frac{-\Delta_j G^0(T,P^o)}{RT}\right] \tag{24}$$

with

$$\Delta_j G^0(T,P^o)=\sum_i \nu_{ij} g_i^0(T,P^o) \tag{25}$$

where ν_{ij} denotes the stoichiometric coefficient of compound i in reaction j, with the sign convention: ν_{ij} is positive for products and negative for reactants.

Values of equilibrium constants for seven of the considered reactions (reactions 1 to 7 in Table 1) are tabulated as function of temperature in the literature (e.g., Ref. [9]). For the remaining two reactions (8 and 9), the equilibrium constants are calculated using the NIST-Webbook [8] enthalpy and entropy temperature functions of the involved compounds.

The problem at hand is again to determine the molar fractions of the twelve species as well as the total number of moles *n* of the gas mixture. To solve for the 13 unknowns we join the three element mass balance equations and the summation equation to the nine equations of column 2 of Table 2. We get so a set of 13 algebraic equations that we solve applying the iterative Gauss-Newton algorithm implemented in the MATHEMATICA© command `FindRoot`.

As can noticed from Table 3, we obtain almost the same results with both equilibrium calculation approaches: Lagrangian multipliers and mass action equations method.

Species	Lagrange method	Equilibrium Constant method	Unconstrained minimization method
N	0.00002	0.00002	0.00002
O	0.01010	0.01011	0.01012
H	0.02465	0.02463	0.02463
NH	$4.35\ 10^{-6}$	$4.34\ 10^{-6}$	$4.34\ 10^{-6}$
NO	0.01627	0.01637	0.01631
NH_2	$3.92\ 10^{-6}$	$3.91\ 10^{-6}$	$3.91\ 10^{-6}$
H_2O	0.47846	0.47854	0.47854
O_2	0.02156	0.02147	0.02147
N_2	0.29731	0.29731	0.29730

H_2	0.08867	0.08858	0.08858
OH	0.06295	0.06300	0.06301
NO_2	0.00001	0.00001	0.00001

Table 3 – Comparison of equilibrium composition calculated by different approaches (Hydrazine combustion).

The solution for the equilibrium constants method can alternatively be attained using a minimization procedure such as that of Levenberg-Marquardt for unconstrained minimization of the objective function F defined as follows:

$$F=\left(K_1(T)-\frac{y_H^2}{y_{H_2}}P\right)^2+\left(K_2(T)-\frac{y_O^2}{y_{O_2}}P\right)^2+\left(K_3(T)=\frac{y_N^2}{y_{N_2}}P\right)^2+\left(K_4(T)=\frac{y_{H_2}^2 y_{O_2}}{y_{H_2O}^2}P\right)^2 \quad (26)$$

With the MATHEMATICA© command `FindMinimum` where this algorithm is implemented the set of molar fractions of the compounds that minimizes F is readily found. Indeed, a minimum of 10^{-23} for F is attained. The obtained values of the mole fractions are identical with those of the equilibrium constant method, as columns 3 and 4 of Table 3 show.

3.1.3 Direct Gibbs Free-Energy Minimization Method

Alternatively, the same problem can be solved using a direct constrained minimization of the Gibbs free energy function

$$G_M(T,P,n_i)=n\sum_{i=1}^{12} y_i\left[\mu_i^o(T,P^o)+RT\ln P+RT\ln y_i\right] \quad (27)$$

subject to the 3 atom balance equations and the summation equation constraints.

In this case, the MATHEMATICA© command `FindMinimum` is used in association with the interior point algorithm. As Table 4 shows, almost the same values of the mole fractions are obtained as for the preceding solution methods.

Species	Lagrange method	Unconstrained minimization method	Constrained minimization method
N	0.00002	0.00002	0.00002
O	0.01010	0.01012	0.01014
H	0.02465	0.02463	0.02475
NH	$4.35\ 10^{-6}$	$4.34\ 10^{-6}$	$4.35\ 10^{-6}$
NO	0.01627	0.01631	0.01628
NH_2	$3.92\ 10^{-6}$	$3.91\ 10^{-6}$	$3.91\ 10^{-6}$
H_2O	0.47846	0.47854	0.47808
O_2	0.02156	0.02147	0.02160
N_2	0.29731	0.29730	0.29723
H_2	0.08867	0.08858	0.08880
OH	0.06295	0.06301	0.06306
NO_2	0.00001	0.00001	0.00001

Table 4 – Results of the constrained minimization method in comparison with the previous solution techniques (hydrazine combustion).

3.2. Propane combustion

Combustion of hydrocarbon fuels with air produces a gaseous mixture composed at least of the following thirteen species: O_2, O, H_2, H_2O, OH, N_2, NO, CO_2, CO, C, H, N, NO_2. We consider the particular case of the combustion of propane with a stoichiometric amount of air,

assumedly composed of 21 vol. % oxygen and 79 vol. % nitrogen. The equilibrium composition of the gaseous product can be easily found using the element potential method.

The Lagrangian function of the mixture writes

$$L=G_M(T,P,n_i)-\lambda_O f_O-\lambda_H f_H-\lambda_N f_N-\lambda_C f_C \tag{28}$$

with

$$G_M(T,P,n_i)=n\sum_{i=1}^{13} y_i\left[\mu_i^o(T,P^o)+RT\ln P+RT\ln y_i\right] \tag{29}$$

where f_O, f_H, f_N and f_C express the atom balance constraints, respectively

$$f_O=10-(y_O+2y_{O2}+y_{NO}+y_{H2O}+y_{OH}+2y_{NO2}++2y_{CO2}+y_{CO})n=0 \tag{30}$$

$$f_H=8-(y_H++2y_{H2O}+2y_{H2}+y_{OH})n=0 \tag{31}$$

$$f_N=10\left(\frac{79}{21}\right)-(y_N+2y_{N2}+y_{NO}+y_{NO2})n=0 \tag{32}$$

$$f_C=3-(y_C+y_{CO}+y_{CO2})n=0 \tag{33}$$

With

$$n=\sum_{i=1}^{13} n_i \tag{34}$$

Similarly to the hydrazine combustion case, we solve now a set of just five algebraic equations (the atom balance equations and the summation equation) for the Lagrange multiliers λ_O, λ_H, λ_N, λ_C and the total molar amount of the mixture, n. Table 5 shows the composition of the gas mixture obtained using the present method in comparison with the NASA method [10] where an iterative successive substitution algorithm involving matrix inversion is applied to minimize the Gibbs free-energy.

As can be noticed the agreement between both methods is almost perfect.

Species	Lagrange method	NASA method

O_2	0.00402	0.00404
O	0.00007	0.00007
H_2	0.00015	0.00015
H_2O	0.09638	0.09640
OH	0.00148	0.00143
N_2	0.71931	0.71931
NO	0.00320	0.00320
CO_2	0.16621	0.16624
CO	0.00917	0.00915
C	$2.2265\,10^{-16}$	<0.00001
H	$5.8416\,10^{-6}$	<0.00001
N	$1.7339\,10^{-8}$	<0.00001
NO_2	$3.6451\,10^{-6}$	<0.00001

Table 5 – Equilibrium composition of the product gas for propane combustion.

4. Sensitivity Analyses

4.1 Haber Synthesis

Ammonia is an essential compound to all biological processes because nitrogen is present in all proteins and related biological molecules. It is also of strategic importance as it is used as refrigerant in cold producing machines and to produce fertilizers and explosives. The world's

production of ammonia in 2019 capped at 235 million tons and it is expected to reach 290 million tons by 2030. We owe the catalytic synthesis of ammonia to the Nobel Prize winner Fritz Haber. The fabrication process of ammonia is performed in two major steps: synthesis gas production and purification, and ammonia synthesis. The reactants, nitrogen and hydrogen, are produced from air and hydrogen containing hydrocarbons, e.g. natural gas. Secondary air reforming of natural gas follows a primary steam reforming. Most of the obtained carbon monoxide is transformed in carbon dioxide, which is then removed. The rest of CO undergoes a methanation process. The ultimate synthesis feedstock is composed of hydrogen and nitrogen as well some inert gases, typically methane and argon.

The industrial process is energy-intensive; it requires high pressures and produces greenhouse gases (*i.e.*CO_2). Hence, recent research work is directed towards the production of "green" ammonia under mild conditions. New routes to ammonia synthesis include thermos-catalytic, electro-catalytic, photo-catalytic and chemical looping processes. Wang and co-workers provide a recent review of the state-of-the-art research in this area [11].

We choose to focus in the present paper on the last step of the Haber-Bosch process for which the feedstock is a mixture of hydrogen and nitrogen.

The synthesis of ammonia is an exothermic reaction:

$$N_2 + 3H_2 \rightleftharpoons 2NH_3 \quad \text{with} \quad \Delta H = -92.44\, kJ/mol \tag{35}$$

The reaction is also associated with a reduction in volume. The implications of these two characteristics of the reaction will be discussed in the text thereafter. The values of the PR EoS binary interaction parameters for this system are provided in Table 6.

	Hydrogen	**Nitrogen**	**Ammonia**
Hydrogen	0	-0.036	0
Nitrogen	-0.036	0	0.222
Ammonia	0	0.222	0

Table 6 – Peng–Robinson EoS Interaction Parameters for the Haber synthesis

The equality constraints, which are based on atomic mass balances, are easily derived:

$$\text{N:} \qquad 2n_{N2} + n_{NH3} = 2 \tag{36}$$

$$\text{H:} \qquad 2n_{H2}+3n_{NH3}=2r \tag{37}$$

r in the last equation is the initial molar ratio of the reactants, $r=\frac{n_{H2}^{i}}{n_{N2}^{i}}$, where superscript i refers the initial number of moles.

Stoichiometric mixture of hydrogen and nitrogen

We consider first the case of stoichiometric reactant mixture, i.e. $r=3$. Figure 1 shows the effect of temperature and pressure on the molar fraction of ammonia in the product mixture. The continuous lines represent calculation results and the markers, industrial data [12]. As can be noticed from Figure 1, the agreement between the two sets of data is excellent for all pressures and temperatures.

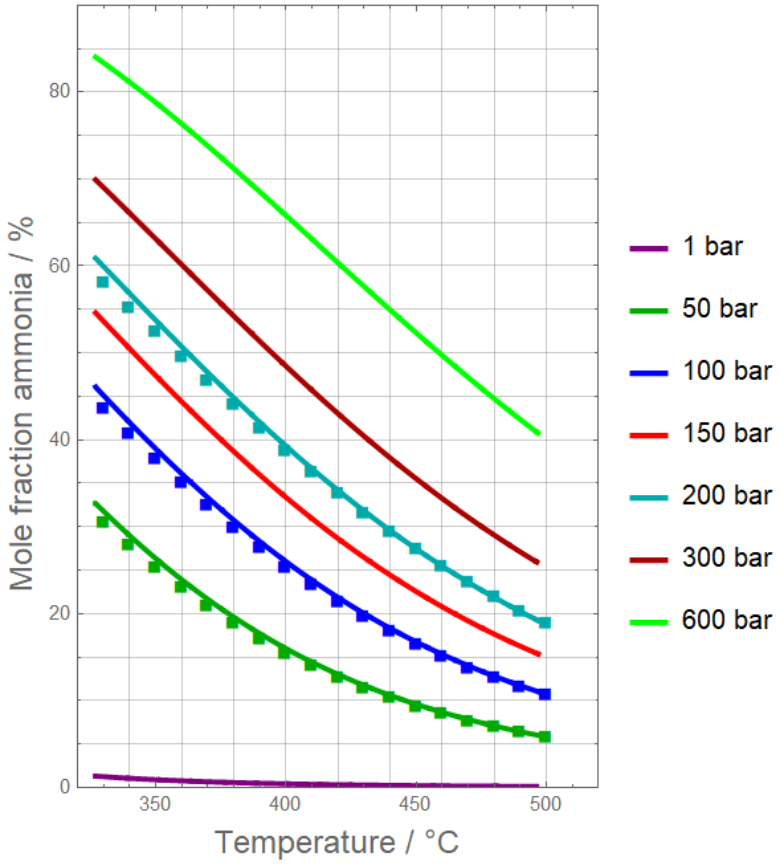

Figure 1 – Equilibrium ammonia mole fraction vs. temperature at various pressures for a gas containing initially a stoichiometric mixture of N_2 and H_2.
Continuous curves: calculated using PR-EoS, Markers: data [12].

.

Figure 2 depicts the nitrogen conversion ratio

$$\chi = \frac{n_{N2}^{i} - n_{N2}^{f}}{n_{N2}^{i}} \tag{38}$$

for the same conditions. Here again, we notice the very good concordance of calculated and experimental data [13].

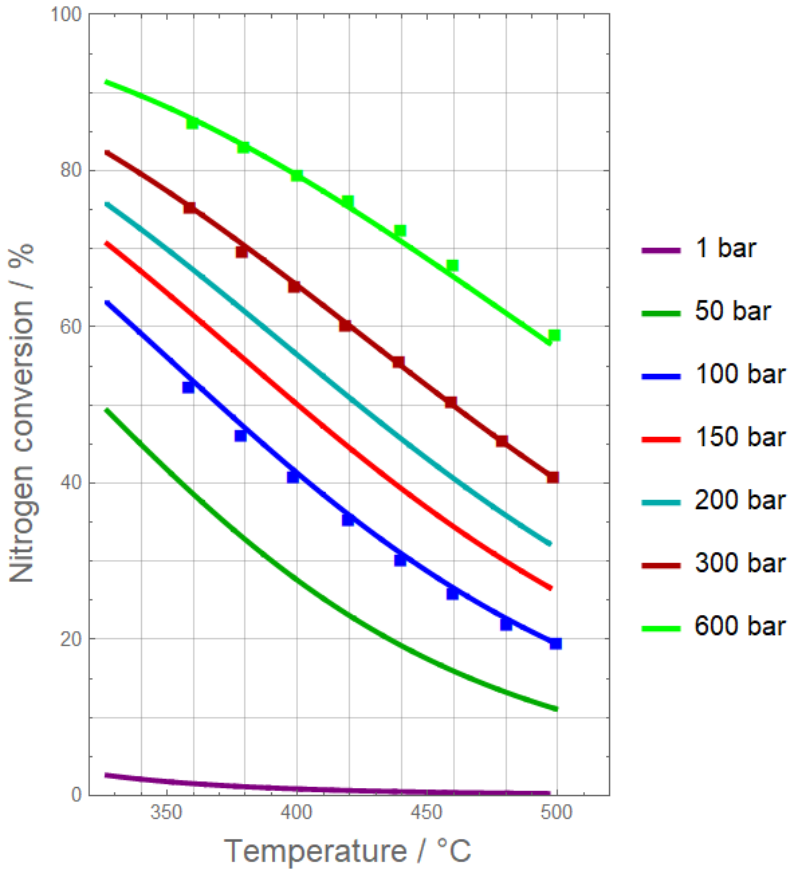

Figure 2 – Equilibrium nitrogen conversion vs. temperature at various pressures for a gas containing initially a stoichiometric mixture of N_2 and H_2.
Continuous curves: calculated using PR-EoS, Markers: data [13].

In accordance with Le Chatelier's principle, the nitrogen conversion is (1) high at lower temperatures since the reaction is exothermic and (2) high for larger pressures since the reaction is associated with a volume reduction. Accordingly, in the industrial ammonia production processes, the pressure ranges frequently between 100 and 300 atm. Some processes are run even at pressures as high as 900 atm. The reaction temperature however is maintained rather high, ranging from 400 to 450°C, to ensure high reaction rates.

The calculated results are obtained using a real gas equation of state, the Peng-Robinson EoS. Figure 3 depicts the compressibility factor of the reacting gas mixture at equilibrium for varying temperatures and pressures. It can be observed that the value of this factor in the considered range of temperature and pressure (1) does not deviate largely from that of an ideal gas, i.e. 1, and (2) increases with increasing temperature and pressure. For a pressure of 100 bars, the compressibility factor is almost constant and equals roughly 1.02 in the temperature range 350°C to 500°C. Under such conditions, the predicted nitrogen conversion ratio assuming ideal gas behavior is in fact in very good agreement with the experimental data as Figure 4 illustrates. For higher pressures (e.g., 300 and 600 bars), the predicted results are very poor: the deviation between calculated and experimental data sets become larger with increasing pressure (see Figure 4).

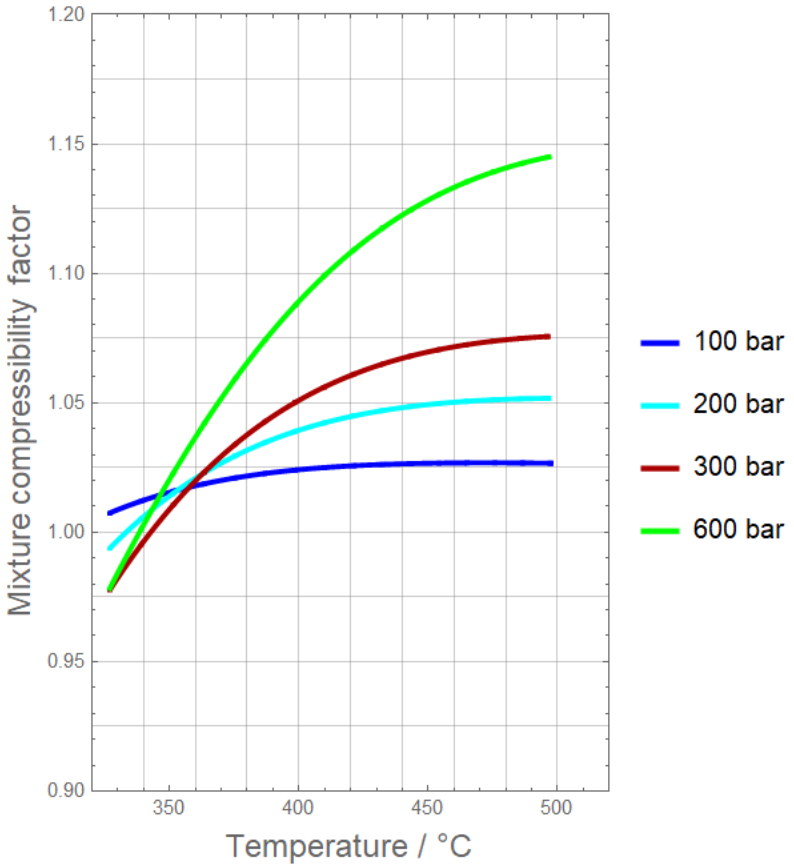

Figure 3 – Mixture compressibility factor *vs*. temperature at various pressures.

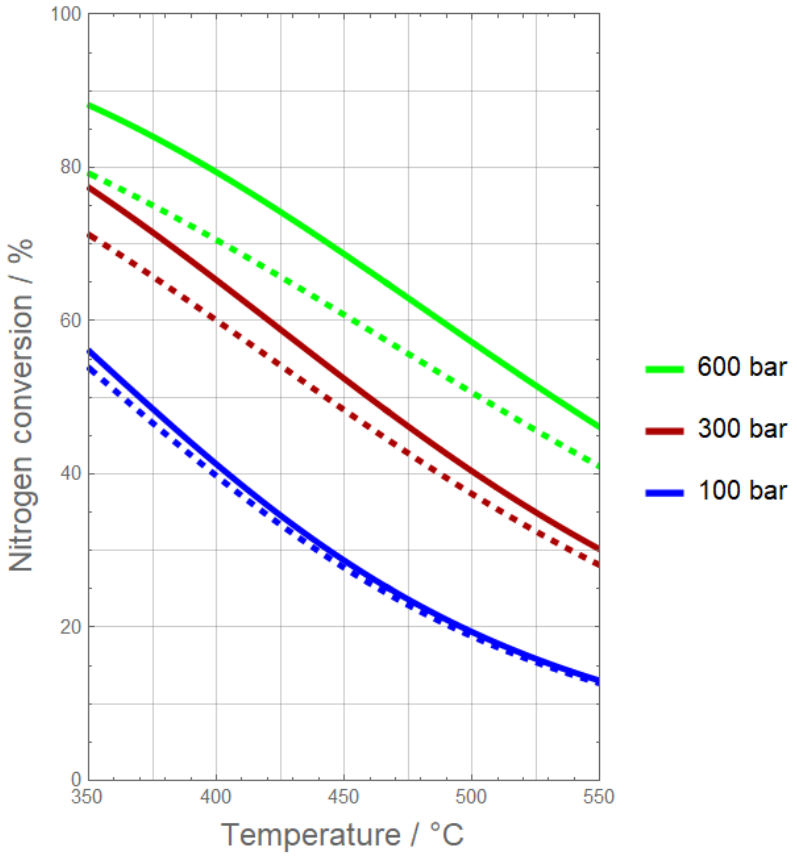

Figure 4 – Calculated equilibrium conversion *vs*. temperature at three different pressures assuming real gas behavior (continuous lines) and ideal gas behavior (dashed lines).

Effect of process gas composition

Figure 5 shows the effect of temperature on the ammonia mole fraction when inert gases are present in the reactants stream. The calculations are performed for a pressure of 100 bars and assuming stoichiometric ratio of the reactants mixed with 10 mol. % inert gases: 7.5% methane and 2.5% argon. The results are benchmarked against industrial data [12] and ASPEN-Plus® simulation results. As can be noticed, all three sets of data are in good concordance.

As expected, the ammonia content of the equilibrium mixture is decreasing with higher temperature but is also decreased by the presence of inert gases, as the comparison with the results depicted in Fig. 1 for the same conditions shows.

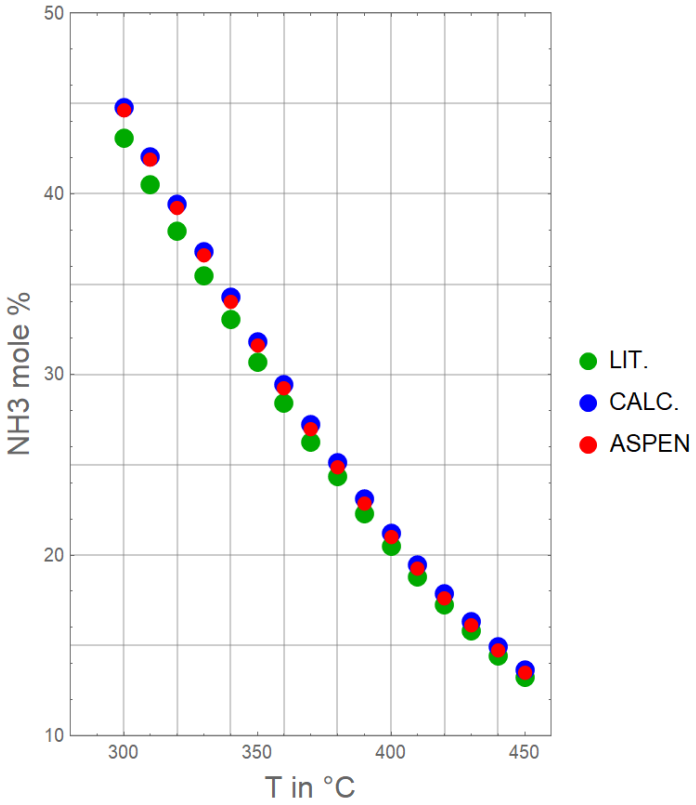

Figure 5 – Equilibrium gas-phase composition vs temperature for a process gas containing initially a stoichiometric mixture of H_2 and N_2 at 100 bars in the presence of inert gases (7.5 mol.% CH4 and 2.5 mol.% Argon). Dots: Red, data obtained from RGIBBS of ASPEN-Plus®, Blue, calculated using PR-EoS, Green, literature data [12]).

Figure 6 depicts the effect of process gas composition r for selected values of temperature by a fixed pressure $P=150$ bars. We notice that for all temperatures the conversion first increases with increasing r, passes by a maximum for $r=3$ and then decreases. Clearly, for $r<3$, there is a deficit in hydrogen. The surplus of nitrogen acts as inert gas: the more of it, the lower the ammonia content in the equilibrium mixture. For $r>3$, the conversion drops due to a deficit in nitrogen. It is now the excess of hydrogen that plays the role of an inert gas, and hence decreases the equilibrium content of the product ammonia.

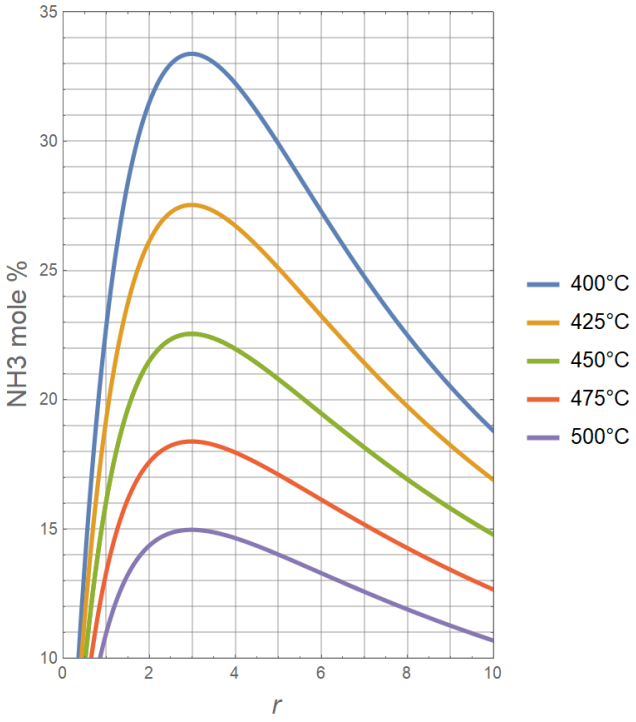

Figure 6 – Equilibrium gas-phase composition for a process gas containing initially r moles ofH_2 for 1 mole ofN_2at various temperatures for $P=150$ ¿.

4.2 Gasification of Glucose using Steam

Biomass gasification is an interesting route to a sustainable energy and chemicals production since biomass is carbon-neutral, renewable and abundant if compared to fossil fuels (gas, petroleum and coal), which are being rapidly depleted [14]. The experimental study of glucose gasification using steam is of importance since glucose represents a simple biomass surrogate [15]. Here, we propose to perform a thermodynamic computation of the equilibrium composition for this gasification process under various conditions. Investigating the operative parameters domain ensures optimal design and operation of a biomass gasifier. In fact, performing experiments on a wide range of operating conditions can be prohibitive because of safety, time and/or cost reasons. Hence, mathematical simulation models and numerical tools are of interest in the prediction of syngas composition and in the optimization of the design and operation of a gasifier. Gasification, involving heterogeneous reactions, are far from the thermodynamic equilibrium due to both low reaction rates and short residence times. Thus, thermodynamic predictions represent target values toward which the experimentalist should always aim.

The overall reaction between glucose and steam can be expressed as follows:

$$C_6H_{12}O_6 + r\,H_2O \rightarrow l\,CO + m\,H_2 + p\,H_2O + q\,CO_2 + v\,CH_4 + w\,C \quad \text{(R.1)} \tag{39}$$

Where r represents the steam/glucose molar ratio and

$$q = \left(3 + \frac{r-l-p}{2}\right);\ v = \left(3 + \frac{r-m-p}{2}\right);\ w = \left(p - r + \frac{m-l}{2}\right) \tag{40}$$

Table 7 lists the possible transformation routes to the gasification products [16, 17]. Among these reactions, we find the coke gasification (R.2), the Boudouard reaction (R.3), the hydrogenating reaction (R.4), the dry reforming of methane (R.5), the steam reforming of methane (R.6) and finally the water gas shift reaction (R.7). For this more complex system, the Gibbs free minimization approach becomes clearly superior to the reaction coordinates – equilibrium constants method. Indeed, it is usually quite challenging to enumerate all chemical reactions involved and to find the expressions for their corresponding equilibrium constants.

Chemical Reaction		$\Delta_R H^0(298\,K)$ $[kJ/mol]$	$K\ (1000\,°C)$
$C + H_2O \leftrightarrows H_2 + CO$	(R.2)	+131.4	7.0401
$C + CO_2 \leftrightarrows 2CO$	(R.3)	+172.6	6.499
$C + 2H_2 \leftrightarrows CH_4$	(R.4)	-75.0	0.049
$CH_4 + CO_2 \leftrightarrows 2CO + 2H_2$	(R.5)	+247	132.013
$CH_4 + H_2O \leftrightarrows CO + 3H_2$	(R.6)	+201.9	169.182
$CO + H_2O \leftrightarrows H_2 + CO_2$	(R.7)	-41.2	1.0051

Table 7 – Main reactions involved in the gasification process of glucose using steam.

Values of the PR EoS binary interaction parameters for commonly encountered compounds in glucose gasification using steam are given in Table 8.

	CH_4	H_2	H_2O	CO	CO_2
CH_4	0	0.2020	0.5000	0.0210	0.1000
H_2	0.2020	0	-0.2998	0.0253	0.1202
H_2O	0.5000	-0.2998	0	-0.3896	0.0445
CO	0.0210	0.0253	-0.3896	0	-0.0314
CO_2	0.1000	0.1202	0.0445	-0.0314	0

Table 8 – Peng-Robinson EoS interaction parameters for biomass gasification products.

Denoting with $n_{CH4}, n_{H2}, n_{H2O}, n_{CO}, n_{CO2} \wedge n_C$ the number of moles at equilibrium of $CH_4, H_2, H_2O, CO, CO_2 \wedge C$, respectively, the equality constraints write:

$$\text{C:} \quad n_{CH4} + n_{CO} + n_{CO2} + n_C = 6 \tag{41}$$

$$\text{H:} \quad 4n_{CH4} + 2n_{H2} + 2n_{H2O} = 12 + 2r \tag{42}$$

$$\text{O:} \quad n_{H2O} + n_{CO} + 2n_{CO2} = 6 + r \tag{43}$$

Effect of pressure and temperature

Figures 7–10 illustrate the effect of pressure on the gasification equilibrium of glucose at $T = 1000\text{K}$ for an initial glucose to steam molar ratio equal to unity (i.e., $r = 1$). The composition of the gas phase vs. pressure is depicted in Fig. 7, the amount of solid carbon formed in Fig.8, the number of moles in the gas phase in Fig. 9 and finally, the H_2/CO molar ratio in Fig. 10. The solid lines in Fig. 7 represent the compositions of $CH_4, H_2, H_2O, CO, \wedge CO_2$ obtained by our calculation using MATHEMATICA© while the colored squares are their counterparts gathered from RGIBBS of ASPEN-Plus®. Figures 7–9 show in accordance with Le Chatelier's principle that increasing the pressure disadvantages the expansive reactions (R.2, R.3, R.5 and R.6 in Table 7) and so lowering the total number of moles in the gaseous mixture, promoting the formation of solid carbon and of the low-energy components $H_2O \wedge CO_2$. At the same time, the production of syngas $(H_2 \wedge CO)$ is largely hindered, even if the ratio H_2/CO is increased (Fig. 10).

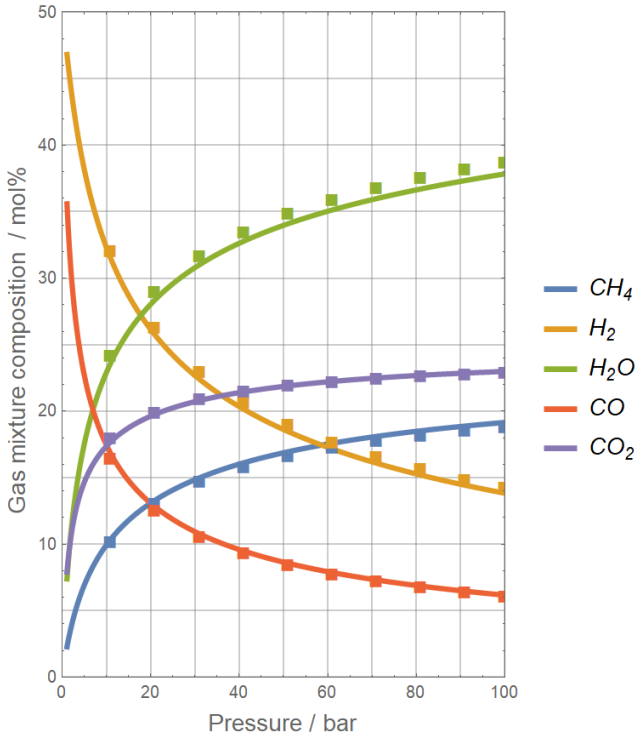

Figure 7 – Equilibrium composition of the gas phase vs. pressure an initial reaction mixture containing 1 mole glucose for 1 mole steam at$T = 1000$ K (solid lines: present calculation, squares: data computed by RGIBBS of ASPEN-Plus®).

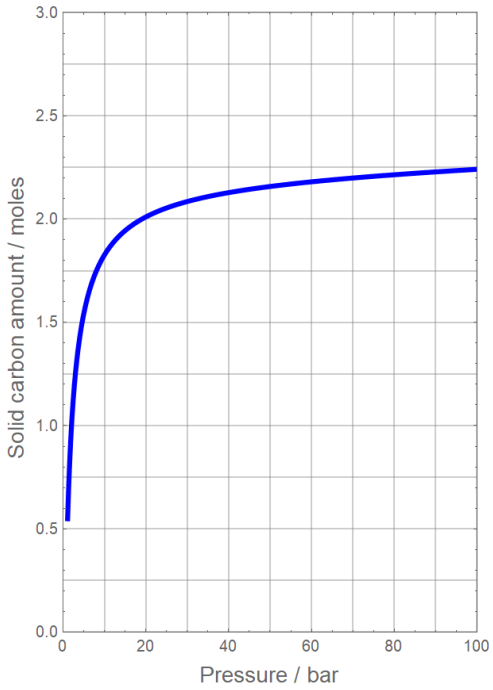

Figure 8 – Solid carbon content vs. pressure for an initial reaction mixture containing 1 mole glucose and 1 mole steam at$T = 1000$ K.

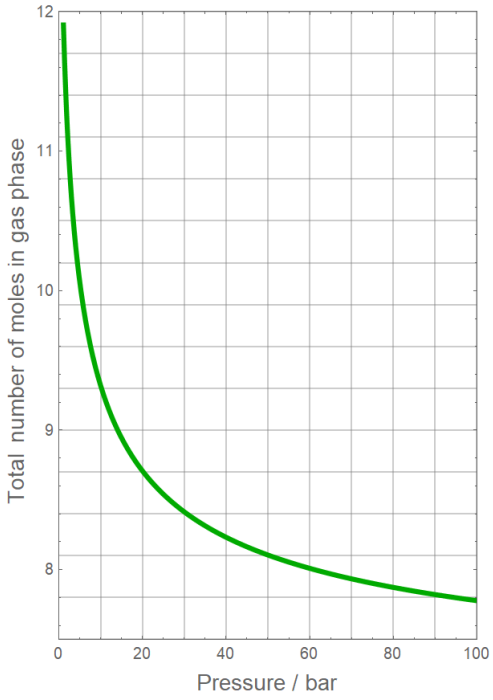

Figure 9 – Evolution of total number of moles in the gas phase vs. pressure for an initial reaction mixture containing 1 mole glucose and 1 mole steam at $T = 1000$ K.

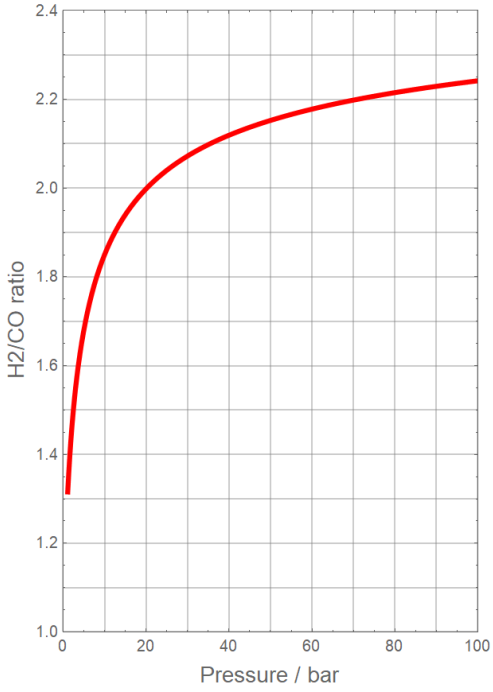

Figure 10 – H2/CO ratio vs. pressure for an initial reaction mixture containing 1 mole glucose for 1 mole steam at $T = 1000$ K.

Figures 11-13 show the effect of temperature on the steam gasification equilibrium of glucose with a reactant molar ratio equal to unity and $P=1$ bar. Again, the solid lines in Fig. 11 represent the mole fractions in the gaseous phase of the different components obtained by our calculation while the colored squares the data obtained from RGIBBS of ASPEN-Plus®. Clearly, the agreement between both methods of calculation is excellent. Figure 12 depicts the evolution of the formed solid carbon, and Fig. 13, that of the total number of moles in the gas phase. Low pressure and higher temperatures are now favoring the expansive and endothermic reactions (R.2, R.3, R.5 and R.6 in Table 7). Consequently,

- The total number of moles in the gas phase is increasing (Fig. 13), and (2) the formation of the syngas components $H_2 \wedge CO$ is becoming predominant with increasing temperature (Fig. 11).

- Further, the amount of solid carbon is rapidly decreasing (Figs. 12) owing to the tar reforming reaction (R.2) and the Boudouard reaction (R.3). In fact, solid carbon is being continuously consumed with increasing temperature until it is totally depleted at $T=760\,°C\,(1034\,K)$. From this temperature upwards, only the reactions R.5, R.6 and R.7 are involved.

- Concomitantly, the steam content of the gas mixture is also decreasing due to the strong endothermic reactions R.2 and R.6 where it is used as reactant.

The similar behavior of the curves representing the mole fractions of CO_2 and CH_4 in Fig. 11 is attributable to the fact that these components are participating in the reacting mixture at the same time as reactants ¿R.3 and R.5 forCO_2; R.5 and R.6 forCH_4¿ and as products ¿R.7 for CO_2; R.4 forCH_4¿.

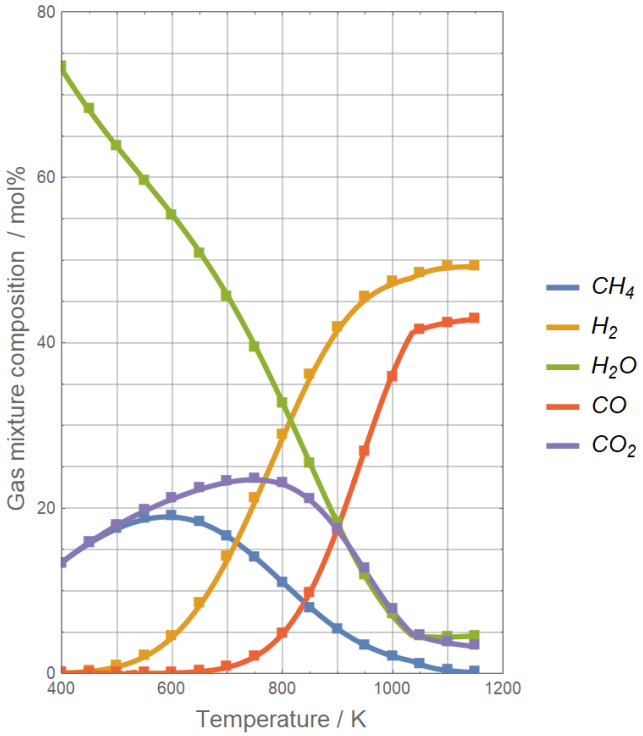

Figure 11 – Equilibrium composition of the gas phase vs. temperature for an initial reaction mixture containing 1 mole glucose for 1 mole steam at$P=1$ bar (solid lines: present calculation, squares: data computed by RGIBBS of ASPEN-Plus®).

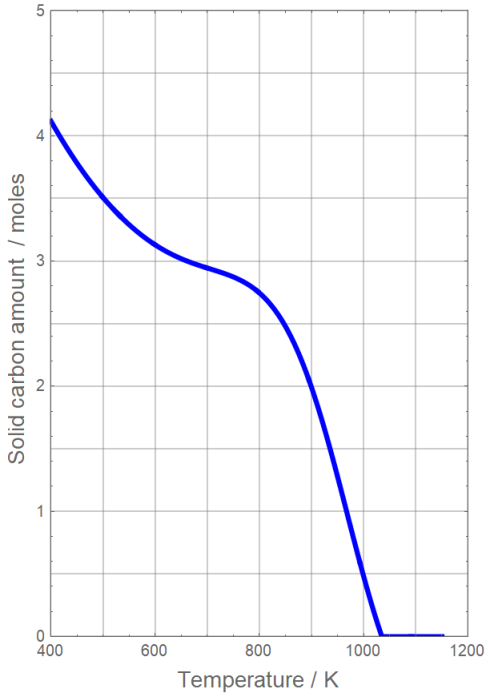

Figure 12 –Solid carbon content vs. temperature for an initial reaction mixture containing 1 mole glucose and 1 mole steam at$P=1$ bar.

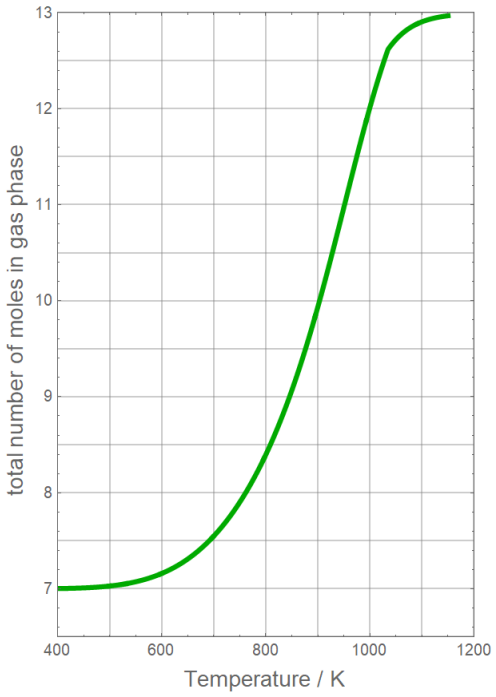

Figure 13 – Evolution of total number of moles in the gas phase vs. temperature for an initial reaction mixture containing 1 mole glucose and 1 mole steam at $P=1$ bar.

Our method is able to reproduce the correct behavior even beyond the temperature where the number of moles of carbon becomes equal to zero (i.e., $n_6=0$). This occurs at a temperature around 1034 K for the present case study when $P=1$ bar and $r=1$. In order to be able to use the Lagrangian multipliers approach, we consider only equality constraints steaming from the material balance equations and drop the inequality ones (i.e., $n_i \geq 0 \, for \, i=1..6$¿. Hence, to obtain the correct behavior beyond $T=1034$ K, we have modified slightly our method in order to implement the inequality condition ensuring that the number of moles must be positive (i.e., $n_6 \geq 0$) by replacing in the coding all occurrences of n_6 by $Max[\{n$¿¿$6,0\}]$¿.

Effect of Glucose/Steam ratio

Figures 14 and 15 depict the effect of the steam to glucose molar ratio, r, on the equilibrium amount of solid carbon and the compositions of the gas phase at $T=1000$ K and $P=1$. We notice the rapid depletion of solid carbon with increasing steam/glucose ratio due to the reforming reaction R.2. Expectedly, the quantity of carbon decreases quasi-linearly with the added amount of steam (Fig. 14). By a ratio of 1.7, all solid carbon has then been consumed. For larger values of r and in the absence of carbon, a source for $CH_4, CO, \wedge CO_2$, and the steady addition of steam, the remaining chemical transformations R.5, R.6 and R.7 leads

eventually to the exhaustion of methane and the continuous consumption of carbon monoxide in favor of carbon dioxide (water-shift reaction R.7). Concurrently, more hydrogen is produced. Fig. 15 illustrates these observations.

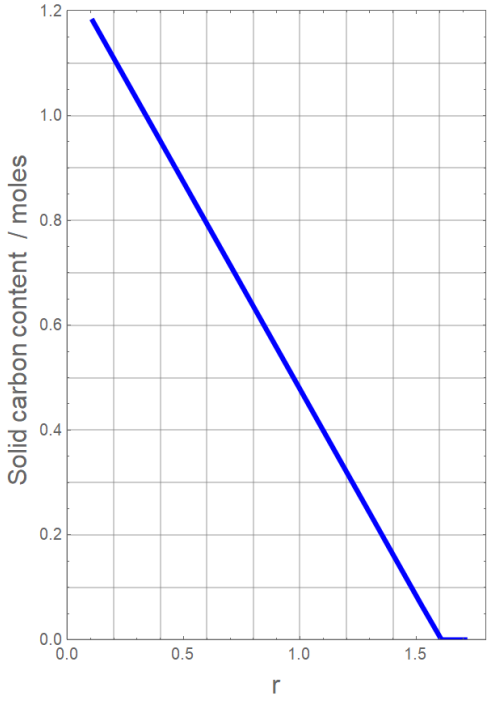

Figure 14 –Solid carbon content vs. water/glucose-ratio at$P=1$ bar and $T=1000$ K.

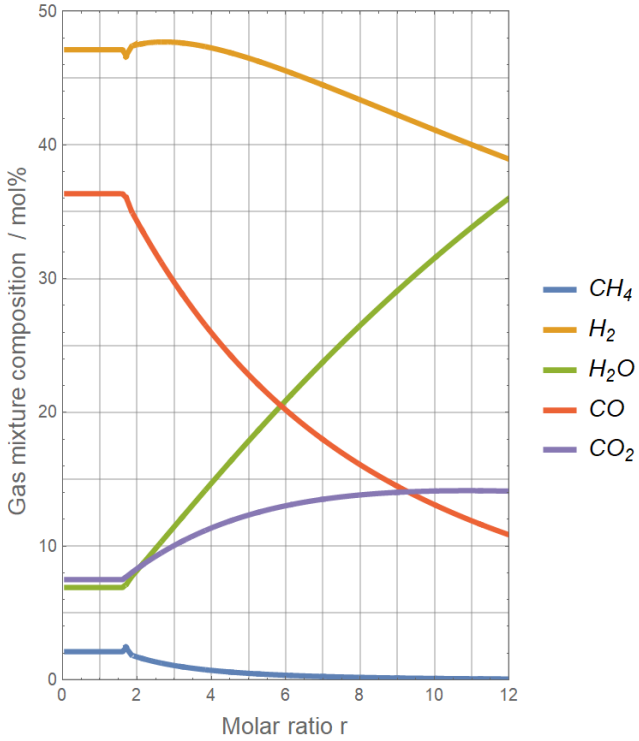

Figure 15 – Effect of water/glucose-ratio on the gas phase composition at $P=1$ bar and $T=1000$ K.

4.3 Gasification of Cellulose using Steam

Cellulose, the most abundant organic polymer, is a structural component of cell wall in green plants. It is a linear polysaccharide with the chemical formula $\left[C_6H_{10}O_5\right]_n$ with n varying from hundreds to thousands.

The overall reaction between cellulose and steam can be expressed by the transformation

$$C_6H_{10}O_5 + r\,H_2O \rightarrow v\,CH_4 + p\,H_2O + l\,CO + q\,CO_2 + w\,C + m\,H_2 \quad \text{(R.8)} \tag{44}$$

Where

$$q = \left(\frac{5+r-l-p}{2}\right);\ v = \left(\frac{5+r-m-p}{2}\right);\ w = \left(1+p-r+\frac{m-l}{2}\right) \tag{45}$$

The equality constraints are easily derived

$$\text{C:} \quad n_{CH4} + n_{CO} + n_{CO2} + n_C = 6 \tag{46}$$

$$\text{H:} \quad 4\,n_{CH4} + 2\,n_{H2} + 2\,n_{H2O} = 10 + 2r \tag{47}$$

$$\text{O:} \quad n_{H2O} + n_{CO} + 2\,n_{CO2} = 5 + r \tag{48}$$

For the elementary steps occurring in the gasification process of cellulose using steam, Table 5 still applies [16, 17].

Effect of pressure and temperature

The effect of pressure and temperature on the gasification equilibrium of cellulose with steam are similar to those already discussed in the preceding case. Figure 16 shows the equilibrium composition versus pressure when the initial cellulose to steam molar ratio is equal to unity and $T = 1000$ K. The solid lines represent the gas-phase water-free mole fractions for $CH_4, H_2, CO \wedge CO_2$ obtained by our calculation using MATHEMATICA© while the colored squares are their counterparts gathered from RGIBBS of ASPEN-Plus®. Clearly, the match between the two sets of data is very good.

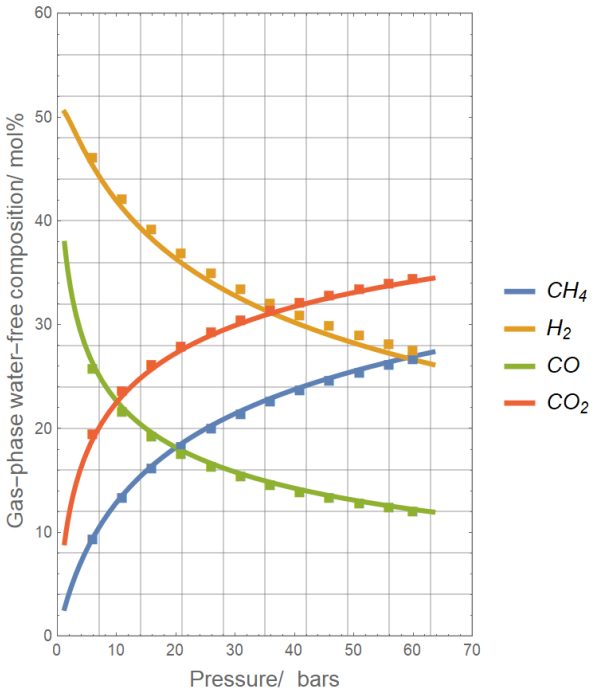

Figure 16 – Equilibrium curves for a gas containing1 *mole of Cellulose* and1 *mole of* H_2O at$T=1000$ K (solid lines: present calculation and squares: data computed by RGIBBS of ASPEN-Plus®)

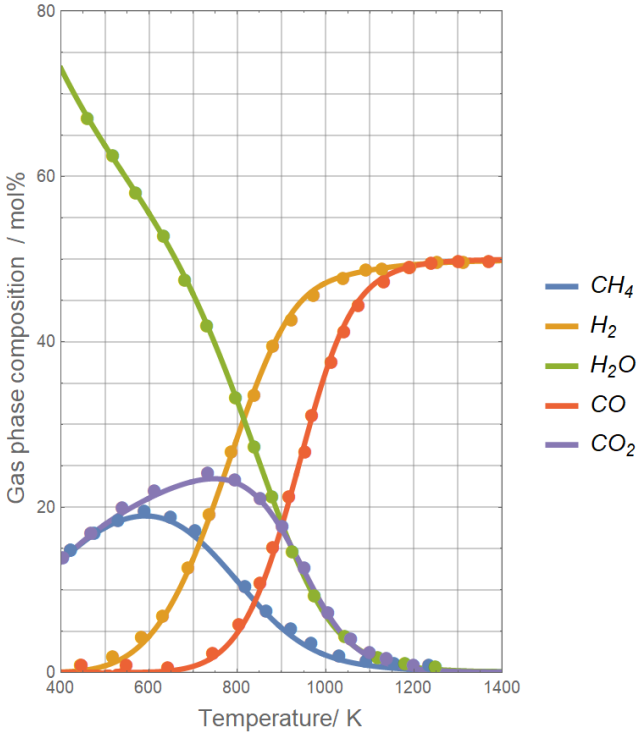

Figure 17 – Equilibrium gas-phase composition vs. temperature at$P=1$ bar for an initial mixture containing 1 mole of water for 1 mole of cellulose (solid lines: present calculation; dots: data obtained from Ref. 18).

Figure 17 provides the equilibrium composition versus temperature when the initial cellulose to steam molar ratio is equal to unity and $P=1$ bar. The solid lines represent the overall mole fractions of the different components obtained by our calculation using MATHEMATICA© while the colored dots are their counterparts gathered from digitizing Figure 1 of Ref. [18]. Again, the match between the two sets of data is excellent. We notice further that high temperatures and low pressures favor the syngas production by the cellulose gasification process, similar to that of glucose gasification process.

Figure 18 depicts the ratio H_2/CO versus T for an initial cellulose to steam molar ratio equals to unity and $P=1$ bar. This ratio decreases with increasing temperature until it reaches unity

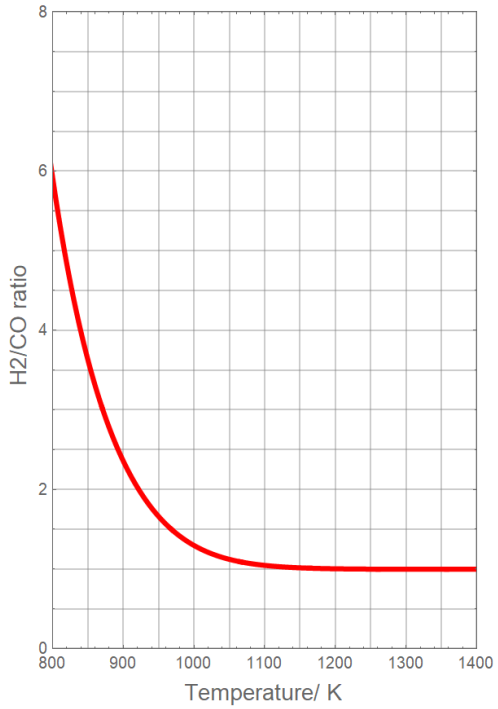

Figure 18 – H_2/CO ratio versus T for an initial mixture containing $1\,mole\,of\,cellulose$ and $1\,mole\,of\,H_2O$ at $P=1$ bar.

Conclusion

The theoretical determination of the equilibrium composition is of particular importance to researchers in academia and industry who prepare new catalysts. Indeed, the gap between

such data and their experimental counterparts is a measure of catalyst performance. In the present paper, we illustrate first by two examples (hydrazine and propane combustion) the various methods that can be applied to calculate complex chemical equilibria under fixed reactant composition, temperature and pressure, in particular the Lagrangian multiplier procedure. This latter method is then used in conjunction with the arc-length continuation technique in order to perform sensitivity analyses, i.e. to determine equilibrium compositions for chemically reacting systems under various conditions and in the presence of gas and/or solid phases. The resulting system of nonlinear algebraic equations is generally complex and any root finding procedure requires a good initial guess for convergence. When performing sensitivity analyses, the arc-length continuation becomes handy. Indeed, to perform parametric studies (i.e., vary temperature, pressure, initial molar ratio…) one does not need to fetch for a good initial guess for every single new set of values of the parameters...

In order to show the breadth of our approach, we study the following three systems:

1- Haber synthesis to produce ammonia,
2- Gasification of glucose using steam to produce syngas,
3- Gasification of cellulose using steam to produce syngas.

For the first case study, in accordance with Le Chatelier's principle, the calculated conversion is (1) high at lower temperatures because the unique reaction involved is exothermic and (2) high for larger pressures because of the volume reductions that accompany the forward reaction. We also discuss the effect of the initial molar ratio of the reacting species on conversion. For the Haber process, as expected, the maximum conversion is obtained when the composition of the initial reacting mixture is stoichiometric.

For the gasification case studies (i.e., the last two case studies), our results clearly indicate that syngas production is favored by low pressures and high temperatures.

Data generated by the present calculations were benchmarked against their counterpart either obtained from the open literature or using RGIBBS of ASPEN-Plus®. For all case studies, very good agreement was observed. In one instance (i.e., when the carbon is depleted), we pinpoint the limitations inherent to our methodology of solution and show how one can overcome such shortcomings in order to satisfy the positivity conditions on our decision variables. It is relatively straightforward to extend the present study to other situations such as:

1- The gas-phase oxidation of sulfur dioxide with oxygen, in the presence or not of nitrogen, to obtain sulfur trioxide (a typical feedstock in the synthesis of sulfuric acid).
2- Naphthalene gasification using either air or pure oxygen.
3- The gasification of cellulose or glucose using supercritical water.
4- The gasification of cellulose or glucose using carbon dioxide – an abundant greenhouse gas – as oxidizing agent. Hence, performing simultaneous biomass gasification and carbon dioxide capture.
5- Based on the plethora of proximate and ultimate analyses of native biomasses available in the open literature (e.g., olive pomace, almonds shells, date seeds…), one can perform gasification calculations analogous to last two case studies reported in the present paper.

Finally, details and coding of our calculations, which were performed using MATHEMATICA© and ASPEN-PLUS®, are available upon request from the corresponding author.

Acknowledgment

The Tunisian Ministry of Higher Education is duly acknowledged for allowing Dr. Housam Binous to take a sabbatical leave in the academic year 2020-2021 in order to complete this paper.

Data Availability Statement

The computer notebooks are available upon request from the corresponding author.

Conflict of Interest

Authors have no conflict of interest relevant to this article.

Appendix A: Peng-Robinson equation of state

The Peng-Robinson Equation of State (PR EoS) was developed primarily for hydrocarbons but can also handle other common compounds of interest such as water, carbon dioxide and monoxide, nitrogen, hydrogen and oxygen [4, 19]. An additional advantage of this cubic EoS resides in its ability to describe both liquid-phase and vapor-phase behavior. This cubic equation relates molar volume v to pressure P and temperature T and writes [4, 19]:

$$P=\frac{RT}{v-b}-\frac{a\alpha(T)}{v(v+b)+b(v-b)} \tag{A-1}$$

where

$$a=0.45724\frac{R^2T_c^2}{P_c},b=0.0778\frac{RT_c}{P_c} \tag{A-2}$$

$$\alpha(T)=\left[1+\left(0.37464+1.54226\,\omega-0.26992\,\omega^2\right)\left(1-\sqrt{T_r}\right)\right]^2 \tag{A-3}$$

and

$$T_r=\frac{T}{T_c} \tag{A-4}$$

The PR EoS can be extended to mixtures using the mixing and combining rules given below [4, 19]:

$$P=\frac{RT}{v_M-b_M}-\frac{a_M}{v_M(v_M+b_M)+b_M(v_M-b_M)} \tag{A-5}$$

With mixture a_M and b_M related to their individual components counterparts by:

$$b_M=\sum_{i=1}^{n}y_ib_i,a_M=\sum_{i=1}^{n}\sum_{j=1}^{n}y_iy_ja_{ij},a_{ij}=\sqrt{a_ia_j}\left(1-k_{ij}\right) \tag{A-6}$$

$$a_i=\frac{0.45724\,\alpha_i(T)R^2T_{ci}^{\,2}}{P_{ci}},b_i=\frac{0.0778\,RT_{ci}}{P_{ci}} \tag{A-7}$$

$$\alpha_i(T)=\left[1+\beta_i\left(1-\sqrt{T_{ri}}\right)\right]^2 \quad with\ \beta_i=0.37464+1.54226\,\omega_i-0.26992\,\omega_i^2 \tag{A-8}$$

and

$$¿T_{ri}=\frac{T}{T_{ci}} \tag{A-9}$$

The binary interaction parameters,k_{ij}, are usually set equal to zero if unavailable [4, 19].

The residual molar Gibbs free energy for pure component is given by [10]:

$$\frac{G^R}{RT}=Z-1-\ln\left(Z-\frac{Pb}{RT}\right)-\frac{a}{2\sqrt{2}bRT}\ln\left(\frac{v+\left(1+\sqrt{2}\right)b}{v+\left(1-\sqrt{2}\right)b}\right) \quad \text{(A-10)}$$

For a mixture, the residual contribution G_M^R is then

$$\frac{G_M^R}{RT}=Z-1-\ln\left(Z-\frac{Pb_M}{RT}\right)-\frac{a_M}{2\sqrt{2}b_M RT}\ln\left(\frac{v_M+\left(1+\sqrt{2}\right)b_M}{v_M+\left(1-\sqrt{2}\right)b_M}\right) \quad \text{(A-11)}$$

The mixture molar volume v_M is determined from the roots of the cubic PR EoS. In the expression of the Gibbs free energy, the numbers of moles of all species present in the gas-phase, n_i, appear implicitly since they are related to the mole fractions by:

$$y_i=\frac{n_i}{n} \quad \text{(A-12)}$$

Up to three values for Z or v_M, which result from solving the PR EoS at specific temperatures and pressures, can be obtained. If two roots of the cubic equation, which has real coefficients, are complex conjugate then there is a single phase in the system (i.e., either a gas or a liquid phase). On the other hand, if all three values are real then we have a two-phase system. In such case, the largest value corresponds to the vapor-phase property (i.e., Z or v_M) while the smallest one is its liquid-phase counterpart [3].

Appendix B: Arc-length Continuation Technique

General Considerations

Let us consider the following parametric system of N nonlinear equations, written in vector representation

$$F(m;\varphi)=0 \quad \text{(B-1)}$$

φ is a parameter on which the solution depends. The components of vectors F and m are respectively, $F=(f_1,f_2,\ldots,f_N)$ and $m=(m_1,m_2,\ldots,m_N)$. The objective is now to obtain a solution of such a system as a continuous function of φ. In the arc-length continuation method, unknown variables and parameter φ are set as a function of the arc-length, represented by s in the following.

Let us now admit that for a particular value φ_0 of the parameter φ, the equations set (11) has a solution m_0,

$$F(m_0;\varphi_0)=0 \quad \text{(B-2)}$$

and that the solution m is an analytic function of φ (i.e. continuous and differentiable). In this case, a neighboring solution $m = m(\varphi)$ can be calculated by constructing a Taylor expansion aboutφ_0. For a multi-value function ofφ, the solution can be parameterized in term of arc-length s on the solution curve. Therefore, we can write:

$$m = m(s), \quad \varphi = \varphi(s) \tag{B-3}$$

So that Eqs. (11) become

$$F(m(s), \varphi(s)) = 0 \tag{B-4}$$

To solve Eq. (14), one more relation is needed. The appropriate auxiliary equation is given by the definition of the arc-length:

$$\frac{dm}{ds} \cdot \frac{dm}{ds} + \left(\frac{d\varphi}{ds} \right)^2 = 1 \tag{B-5}$$

The system to solve (14) and (15) is now a differential algebraic equations (DAE) set in $(N+1)$ unknowns. Although, one can solve this DAE using the built-in MATHEMATICA© function `NDSolve` [20], we choose in the present article to discretize Eq. (15) [21–24]. The resulting algebraic system is then solved with the built-in MATHEMATICA© function `FindRoot` in combination with the continuation procedure `NestList`. This latter MATHEMATICA© function is very handy when one wishes to make an iterative computation using every previously found solution as a starting point for the next iteration or equilibrium calculation.

Application to Reacting Systems

Temperature or pressure parametric study

In order to study the effect of temperature, we fix the pressure ($e.g., P = P_0$) and consider temperature as a parameter. The system of nonlinear equations, given by Eq. (X), can be written in vectorial form as

$$F(m; \varphi) = 0$$

where $\varphi = T$ and $m = ¿¿$) is a vector of dimension$(N + w + 2)$. Hence, we have formed the DAE to be solved using `FindRoot` in conjunction with `NestList` as indicated in the previous section.

The effect of pressure is studied using a similar approach to the description given in the paragraph above. This time, we fix the temperature ($e.g., T = T_0$) and consider pressure as a parameter (i.e., we set$\varphi = P$ ¿.

Initial composition parametric study

In order to study the effect of the initial composition of the reacting system, we fix both the pressure and temperature ($e.g., P = P_0 \wedge T = T_0$) and consider the initial number of moles of one of the components of the system,r, as a parameter. The system of nonlinear equations, given by Eq. (X), can be written in vectorial form as $F(m; \varphi) = 0$ where $\varphi = r$ and $m = ¿¿$) is a vector of dimensions$(N + w + 2)$. This latter step requires an appropriate adjustment of the parameters:A_k. Again, we have obtained the DAE to be solved using `FindRoot` in conjunction with `NestList` as indicated previously.

References

[1] van Zeggeren F., Storey S.H., The Computation of Chemical Equilibria, Cambridge University Press, 1970.

[2] Tester JW, Modell M, Thermodynamics and Its Applications (3rd ed.), Upper Saddle River: Prentice Hall, 1996.

[3] Smith JM, Van Ness HC, Abbot MM, Introduction to chemical engineering thermodynamics (7th ed.), New York: McGraw-Hill Higher Education, 2005.

[4] Sandler SI, Chemical and engineering thermodynamics (3rd ed.), Wiley, NY, 1999.

[5] Barin I, Thermochemical Data of Pure Substances, 3rd ed., Weinheim: VCH Verlagsgesellschaft, 1995.

[6] White WB, Johnson SM, Dantzig GB, Chemical Equilibrium in Complex Mixtures, *Journal of Chemical Physics*, 1958; 28(5):751-755.

[7] Reynolds WC, The Element Potential Method for Chemical Analysis, Department of mechanical engineering, Stanford University, January 1986.

[8] NIST Chemistry WebBook, SRD 69, Thermophysical Properties of Fluid Systems, https://webbook.nist.gov/chemistry/fluid/ (accessed December 2020).

[9] Borgnakke C., Sonntag R.E., Fundamentals of Thermodynamics, Wiley, 2013.

[10] Gordon S., McBride B. J., Computer Program for Calculation of Complex Chemical Equilibrium Compositions, Rocket Performance, Incident and Reflected Shocks, and Chapman-Jouguet Detonations. NASA SP-273, 1971.

[11] Wang Q., Guo J., Chen P., Recent progress towards mild-condition ammonia synthesis, *Journal of Energy Chemistry*, 2019; 36:25-36.

[12] Appl M., Ammonia: Principles and Industrial Practice, Weinheim: Wiley-VCH Verlag, 1999.

[13] Gmehling J., Kleiber M., Kolbe B., and Rarey J., Chemical Thermodynamics for Process Simulation, 2nd ed., Weinheim: Wiley-VCH Verlag, 2019.

[14] Kumar A, Jones DD, Hanna MA, Thermochemical Biomass Gasification: A Review of the Current Status of the Technology, *Energies*, 2009; 2(3):556-581.

[15] Adamu S., Binous H., Razzak S.A., Hossain M.M., Enhancement of glucose gasification by Ni/La2O3-Al2O3 towards the thermodynamic extremum at supercritical water conditions, *Renewable Energy*, 2017;111(C):399-409.

[16] Barisano D., Canneto G., Nanna F., Villone A., Alvino E., Carnevale M., Pinto G., Production of gaseous carriers via biomass gasification for energy purposes, *Energy Procedia*, 2014; 45: 2-11.

[17] Lee D.H., Hydrogen production via the Kværner process and plasma reforming, Chapter 12, Editors: Velu Subramani, Angelo Basile, T. Nejat Veziroğlu, In Woodhead Publishing Series in Energy, Compendium of Hydrogen Energy, Sawston: Woodhead Publishing, 2015.

[18] Hathaway B.J., Kittelson D.B., Davidson J.H., Development of a molten salt reactor for solar gasification of biomass, *Energy Procedia*, 2014; 49:1950-1959.

[19] Peng DY, Robinson DB, A New Two-Constant Equation of State, *Indust. and Eng. Chemistry: Fundamentals*, 1976;15(1):59–64.

[20] Binous H, Shaikh AA. Introduction of the arc-length continuation technique in the chemical engineering graduate program at kfupm, *Computer Applications in Engineering Education*, 2015;23(3):344-351.

[21] Binous H, Mejbri K, Bellagi A, Application of graduate-level numerical tools to teach phase equilibria of liquid ternary systems, Computer Applications in Engineering Education, March 2021, doi: 10.1002/cae.22411

[22] H. Binous and A. Bellagi, Calculation of ternary liquid-liquid equilibrium data using arc-length continuation, Eng. Rep. 3(2021), no.2., doi: 10.1002/eng2.12296

[23] Keller HB, Numerical solution of bifurcation and nonlinear eigenvalue problems, Applications of bifurcation theory, P. Rabinowitz (Ed.), New York: Academic Press, 1977.

[24] Doedel EJ, Lecture notes on numerical analysis of nonlinear equations. Numerical continuation methods for dynamical systems, path following and boundary value problems, B. Krauskopf, H. M.Osinga, J. Galán-Vioque (eds.), Dordrecht: Springer, 2007.